INTERNATIONAL JOURNAL OF Electroactive Materials

Int. J. Electroactive Mater. **5 (2017) 1-5**
www.electroactmater.com

RECEIVED
11 January 2017

REVISED
21 January 2017

ACCEPTED FOR PUBLICATION
23 January 2017

PUBLISHED
11 February 2017

Synthesis of Reduced Graphene Oxide and Its Application as Counter Electrode in Dye-sensitized Solar Cell

A.S. Sulaiman, M.Y.A. Rahman*, A.A. Umar

Institute of Microengineering and Nanoelectronics (IMEN), Universiti Kebangsaan Malaysia, 43600, Bangi, Selangor, Malaysia
E-mail: mohd.yusri@ukm.edu.my*

ABSTRACT: Reduced graphene oxide (rGO) was prepared by using modified Hummers' method as an alternative to costly platinum as a counter electrode for dye-sensitized solar cell (DSSC). The effect of weight percentage (wt.%) of GO on the morphology and performance of the DSSC has been investigated. The rGO samples were prepared with various wt.% GO, namely, 0.5, 1.5, 2.5, 3.5 and 4.5 wt.%. The field emission scanning electron microscopy (FESEM) images of the rGO reveal the presence of conductive and non-conductive regions represented by dark region and white strips, respectively. These rGO samples were applied in the DSSC of ITO/TiO_2-N719/electrolyte/rGO. The DSSC using the 0.5 wt.% GO sample performed the highest photovoltaic parameters with the J_{sc}, V and η of 0.68 mA cm^{-2}, 0.56 V and 0.06%, respectively due to the highest electronic conductivity.
Keywords: Counter electrode, DSSC, Hummers method, Reduced graphene oxide

1. Introduction

Graphene has become a popular material for its unique electronics properties such as high electron mobility [1,2], high heat transfers and cost effectiveness [3]. It has been utilized in various electronic devices such as organic field effect transistor (OFET), sensor, organic light emitting diode (OLED) and solar cell as current collector or counter electrode. Reduced graphene oxide (rGO) also becomes as an alternative to replace costly platinum as counter electrode in DSSC since it possesses good electrical conductivity and high surface area [4]. Various ways have been employed to thermally or chemically prepare reduced graphene oxide (rGO) films [5]. The thermal techniques include temperature annealing [6] and UV–assisted photocatalytic reduction [7]. The chemical techniques use reducing agent such as hydrazine or $NaBH_4$ [8].

In this paper, rGO was prepared by using modified Hummers' method and utilized as counter electrode in DSSC. The originality of the work is to synthesize reduced graphene oxide (rGO) film as counter electrode in DSSC. The objective of the work is to investigate the effect of GO composition in term of its weight percentage on the morphology of rGO and the performance parameters of the DSSC utilizing rGO counter electrode such as short-circuit current density (J_{sc}) and power conversion efficiency (η).

2. Experimental

GO flakes was prepared by using the modified Hummers' method. GO flakes with 0.5 wt.% equivalent with 0.5 mg were diluted with deionized water (DI water) and then underwent sonication process for 30 minutes. The solution was stirred for 2 hours to reduce GO to rGO. ITO substrates were cleaned using a standard cleaning procedure in acetone, 2-propanol and ethanol for 15 minutes in ultrasonic bath, respectively. The substrates were then dried under nitrogen flow. The cleaned substrate was spin-coated with 0.5 wt.% rGO solution at 3500 rpm to get well-distributed thin film and heated in vacuum at 0.08 bar at 100 ^oC for 1 hour. All rGO samples have been applied in DSSC as counter electrode. These procedures were repeated for preparing the samples with 1.5, 2.5, 3.5 and 4.5 wt.% GO, respectively.

The TiO_2 films were prepared via liquid phase deposition technique. The TiO_2 samples were sensitized with N719 dye. The morphology of the samples was determined by FESEM instrument (SU8030 Hitachi). The devices were assembled using the sealing technique by sandwiching the TiO_2 coated N719 photoanode and rGO counter electrode. The sandwiched structure was then heated for 5 minutes at 100 ^oC to make sure the sealing layers are tightly assembled. The electrolyte of 0.5 M LiI/0.05 M I_2/0.5 M TBP in acetonitrile was finally injected into the sandwiched structure to form DSSC. The performance study of the DSSC utilizing the samples with various wt.% of GO was carried out by observing the current-voltage under illumination using AM 1.5 simulated light with an intensity of 100 mW cm^{-2} and recorded by Keithley high-voltage source model 237. The photovoltaic measurement for the DSSC utilizing each rGO sample was repeated 5 times. The best photovoltaic parameters are illustrated in **Table 1**.

3. Results and discussion

Fig. 1 shows the FESEM images of the rGO samples prepared from various wt.% GO. From the images, the morphology of the sample changes with GO composition. At 0.5 wt.%, the sample fully contains dark region signifying the sample is highly conductive. Once the composition was increased to 1.5 wt.%, the white strips representing non-conductive region appears [9]. Once the composition was further increased to 2.5 wt.%, the number of white strip decreases compared with the 1.5 wt.% sample. For 3.5 wt.% sample, the number of its white strip is higher than that of 2.5 wt.% sample. It is noticeable that from **Fig. 1 (e)**, the 4.5 wt.% sample has quite similar number of strip to the 3.5 wt.% sample. However, the width of its strips is bigger than the 3.5 wt.% sample. Comparing **Fig. 1 (e)** with the other figures, it is found that the 4.5 wt.% has the widest strip indicating that it has the lowest electrical conductivity.

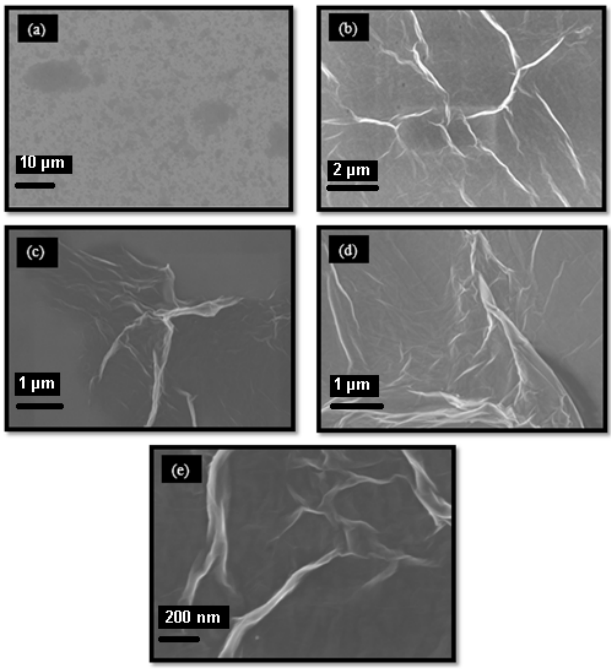

Figure 1: FESEM images of rGO films with various wt.% GO: (a) 0.5 wt.%, (b) 1.5 wt.% (c), 2.5 wt.%, (d) 3.5 wt.% and (e) 4.5 wt.% (10000× magnification)

Fig. 2 illustrates the *I-V* curves in dark for the devices utilizing rGO samples with various wt.% GO. It is found that the reverse bias current for all devices is higher than that in the forward bias. The current in reverse bias is also called leak current. With high leak current and small current in the forward bias, the device will generate small photocurrent and consequently produces small power conversion efficiency upon light illumination [10]. Also, from the figure, it is found that the dark current changes with wt.% GO. However, the increasing or decreasing trend is not observed in the behavior of dark current with wt.% GO. It is noticeable that the device utilizing 4.5 wt.% GO possesses the lowest dark current and that utilizing 0.5 wt.% GO demonstrates the highest dark current.

Fig. 3 shows the Nyquist plots for the dye-sensitized solar cell (DSSC) utilizing rGO prepared from various wt.% GO. Two resistances are found and analyzed from the plots which are bulk resistance (R_b) and charge transfer resistance (R_{ct}) at the interfaces of the devices. R_b is represented by R_1. R_{ct} is represented by R_2 and R_3. All resistances are shown in the equivalent circuit shown in the inset of **Fig. 3**. However, R_4 does not appear in the Nyquist plots in **Fig. 3** since it only shows 2 semicircles. All resistances are illustrated in **Table 1**. From the table, the device with 4.5 wt.% has the highest R_b and R_{ct} and 1.5 wt.% has the lowest R_b and R_{ct}. The device with the lowest R_b and R_{ct} transports charge the fastest from TiO_2 nanoparticles to rGO counter electrode and from the electrolyte to TiO_2 nanoparticles respectively [11].

Table 1: Photovoltaic parameters of DSSC with various GO compositions

wt.%	J_{sc} (mA cm^{-2})	V_{oc} (V)	η (%)	*FF*	R_b (Ω)	R_{ct} (Ω)
0.5	0.68	0.56	0.06	0.17	27.7	36.6
1.5	0.43	0.51	0.03	0.14	25.9	32.1
2.5	0.48	0.52	0.04	0.14	30.5	40.3
3.5	0.42	0.51	0.03	0.14	28.5	40.0
4.5	0.35	0.49	0.02	0.14	36.2	57.0

The current density-voltage (*J-V*) curves for the DSSCs with various wt.% GO under illumination of light are shown in **Fig. 4**. From the figure, it is noticeable that the curves are almost linear signifying that the internal resistance of each device is high. This leads to the small *FF* as illustrated in **Table 1**. The other photovoltaic parameters were analyzed from the figure and illustrated in **Table 1**. From the table, it can be concluded that the device with 0.5 wt.% GO performs the highest photovoltaic parameters. This might be due to the rGO sample prepared from 0.5 wt.% GO has the highest electronic conductivity as shown in the FESEM image in **Fig. 1 (a)**. On the other hand, the device utilizing the 4.5 wt.% sample demonstrated the lowest photovoltaic parameters. This might be caused this device has the highest R_b and R_{ct} as illustrated in **Table 1**. Furthermore, the 4.5 wt.% sample possesses the lowest electronic conductivity as shown in **Fig. 1(e)**. Generally, the highest η that is 0.06% from this work is low. This might be caused by the high leak current as shown in **Fig. 2**. High leak current caused more power loss generated in the device and consequently lowered down its power conversion efficiency.

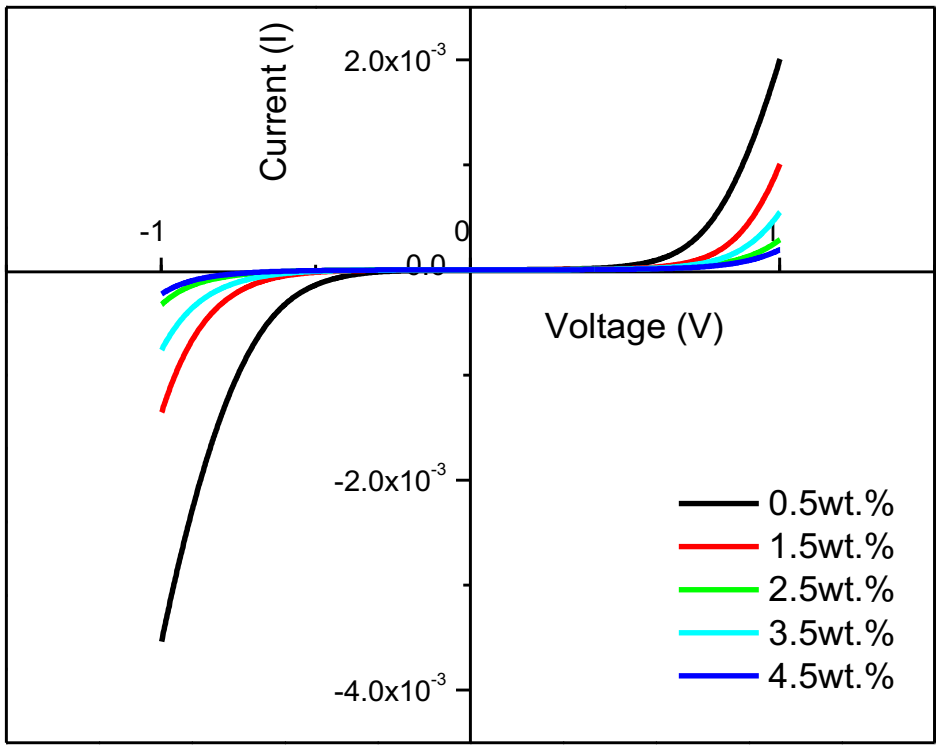

Figure 2: *I-V* curves in dark for the DSSCs with various wt.% GO

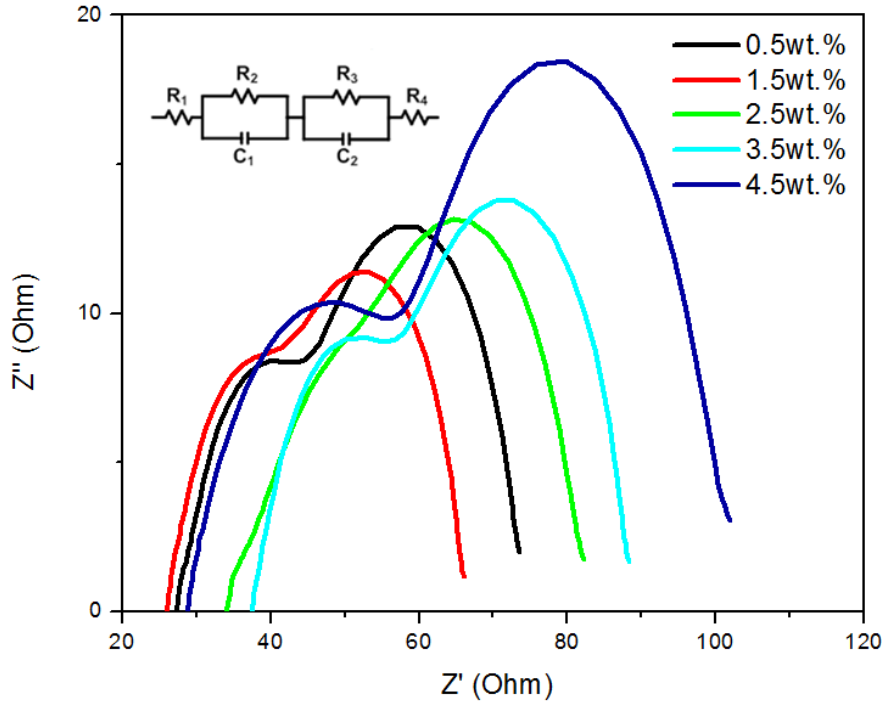

Figure 3: Nyquist plots of DSSCs with difference wt.% GO

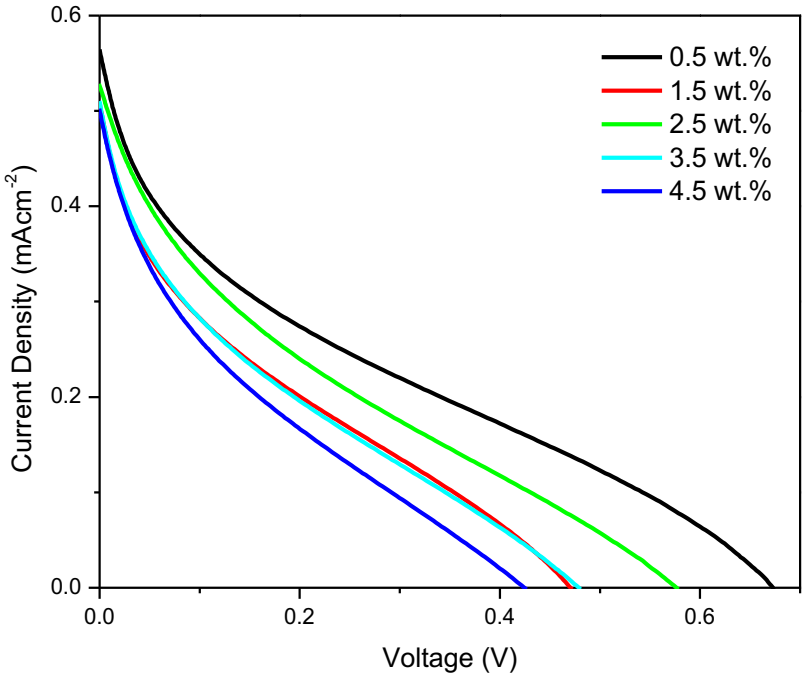

Figure 4: *J-V* curves under the illumination of 100 mWcm^{-2} light for the DSSCs with difference wt.% GO

4. Conclusions

Reduced graphene oxide (rGO) films has been successfully prepared and applied as a counter electrode in the DSSC. The samples contain conductive and non-conductive regions represented by black region and white strips, respectively revealed by FESEM images. The best photovoltaic parameters with the J_{sc} of 0.68 mA cm^{-2} and η of 0.06% was obtained from the device utilizing the rGO sample prepared from 0.5 wt.% GO. This due to this sample possesses the highest electronic conductivity.

Acknowledgement

This work was supported by Universiti Kebangsaan Malaysia under research grant DLP-2015-003.

References

1. J. Yao, X.P. Shen, B. Wang, H.K. Liu, G.X. Wang, Electrochem. Commun. 11 (2009) 1849-1852.
2. L.P. Xue, C.F. Shen, M.B. Zheng, H.L. Lu, N.W. Li, G.B. Ji, L.J. Pan, J.M. Cao, Mater. Lett. 65 (2011) 198-200.
3. A.K. Geim, K.S. Novoselov, Nat. Mater. 6 (2007) 183-181.
4. Z. Wang, P. Li, Y. Chen, J. He, J. Liu, W. Zhang, Y. Li, J. Power Sources 263 (2014) 246-251.
5. G. Eda, G. Fanchini, M. Chhowalla, Nat. Nanotech. 3 (2008) 270-274.
6. M.J. McAllister, Chem. Mater. 19 (2007) 4396-4404.
7. G. Williams, B. Seger, P.V. Kamat, ACS Nano 2 (2008) 1487-1491.
8. S.R. Kim, Md.K. Parvez, M. Chhowalla, Chem. Phys. Lett. 483 (2009) 124-127.
9. M.Y.A. Rahman, A.S. Sulaiman, A.A. Umar, M.M. Salleh, J. Mater. Sci.: Mater. Electron. 28 (2017) 1674-1678
10. M.Y.A. Rahman, L. Roza, A.A. Umar, M.M. Salleh, Int. J. Electroactive Mater. 3 (2015) 15-19.
11. M.Y.A. Rahman, L. Roza, A.A. Umar, M.M. Salleh, J. Alloy Compd. 648 (2015) 86-91.